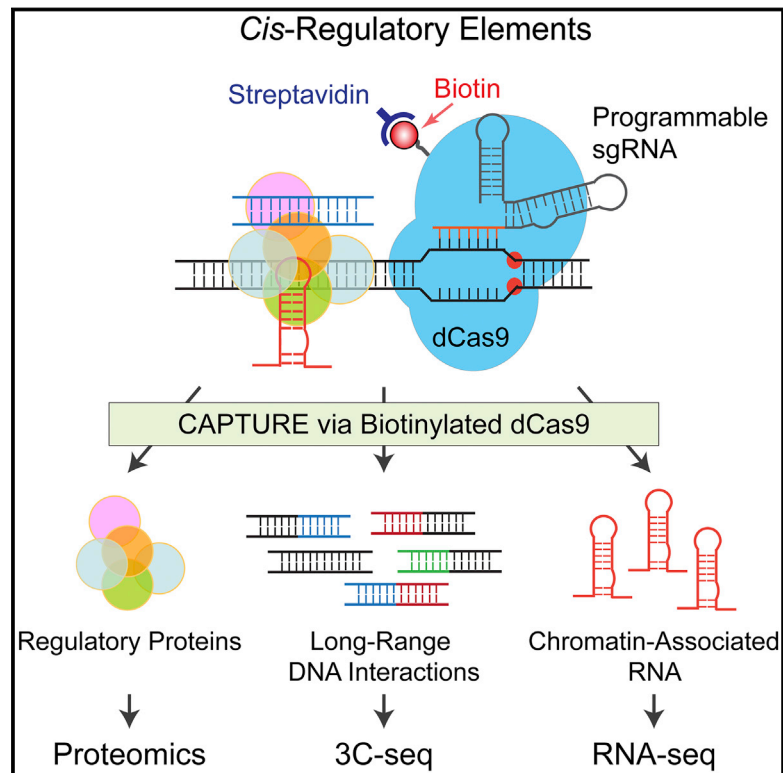


# In Situ Capture of Chromatin Interactions by Biotinylated dCas9

## Graphical Abstract



## Authors

Xin Liu, Yuannu Zhang, Yong Chen, ...,  
Michael Q. Zhang, Zhen Shao, Jian Xu

## Correspondence

zhou\_feng@fudan.edu.cn (F.Z.),  
jian.xu@utsouthwestern.edu (J.X.)

## In Brief

A biotinylated dCas9-based method for simultaneously studying long-range DNA interactions and chromatin-associated proteins at any genomic location.

## Highlights

- dCas9 capture enables analysis of locus-specific chromatin-regulating proteome
- dCas9 capture identifies high-resolution locus-specific long-range DNA interactions
- Capture of disease-associated CREs uncovers mechanisms for  $\beta$ -globin disorders
- Capture of super-enhancers reveals composition-based hierarchical structure



# In Situ Capture of Chromatin Interactions by Biotinylated dCas9

Xin Liu,<sup>1,7</sup> Yuannu Zhang,<sup>1,7</sup> Yong Chen,<sup>2,7</sup> Mushan Li,<sup>3,7</sup> Feng Zhou,<sup>4,7,\*</sup> Kailong Li,<sup>1</sup> Hui Cao,<sup>1</sup> Min Ni,<sup>1</sup> Yuxuan Liu,<sup>1</sup> Zhimin Gu,<sup>1</sup> Kathryn E. Dickerson,<sup>1</sup> Shiqi Xie,<sup>5</sup> Gary C. Hon,<sup>5</sup> Zhenyu Xuan,<sup>2</sup> Michael Q. Zhang,<sup>2,6</sup> Zhen Shao,<sup>3</sup> and Jian Xu<sup>1,8,\*</sup>

<sup>1</sup>Children's Medical Center Research Institute, Department of Pediatrics, University of Texas Southwestern Medical Center, Dallas, TX 75390, USA

<sup>2</sup>Department of Biological Sciences, Center for Systems Biology, University of Texas at Dallas, Richardson, TX 75080, USA

<sup>3</sup>Key Laboratory of Computational Biology, CAS-MPG Partner Institute for Computational Biology, Shanghai Institutes for Biological Sciences, Chinese Academy of Sciences, Shanghai 200031, China

<sup>4</sup>Liver Cancer Institute, Zhongshan Hospital, Key Laboratory of Carcinogenesis and Cancer Invasion, Minister of Education, and Institutes of Biomedical Sciences, Fudan University, Shanghai 200032, China

<sup>5</sup>Cecil H. and Ida Green Center for Reproductive Biology Sciences, Department of Obstetrics and Gynecology, University of Texas Southwestern Medical Center, Dallas, TX 75390, USA

<sup>6</sup>MOE Key Laboratory of Bioinformatics; Bioinformatics Division and Center for Synthetic and Systems Biology, TNLIST; Department of Automation, Tsinghua University, Beijing 100084, China

<sup>7</sup>These authors contributed equally

<sup>8</sup>Lead Contact

\*Correspondence: zhou\_feng@fudan.edu.cn (F.Z.), jian.xu@utsouthwestern.edu (J.X.)  
<http://dx.doi.org/10.1016/j.cell.2017.08.003>

## SUMMARY

**Cis-regulatory elements (CREs) are commonly recognized by correlative chromatin features, yet the molecular composition of the vast majority of CREs in chromatin remains unknown. Here, we describe a CRISPR affinity purification *in situ* of regulatory elements (CAPTURE) approach to unbiasedly identify locus-specific chromatin-regulating protein complexes and long-range DNA interactions. Using an *in vivo* biotinylated nuclease-deficient Cas9 protein and sequence-specific guide RNAs, we show high-resolution and selective isolation of chromatin interactions at a single-copy genomic locus. Purification of human telomeres using CAPTURE identifies known and new telomeric factors. *In situ* capture of individual constituents of the enhancer cluster controlling human  $\beta$ -globin genes establishes evidence for composition-based hierarchical organization. Furthermore, unbiased analysis of chromatin interactions at disease-associated *cis*-elements and developmentally regulated super-enhancers reveals spatial features that causally control gene transcription. Thus, comprehensive and unbiased analysis of locus-specific regulatory composition provides mechanistic insight into genome structure and function in development and disease.**

## INTRODUCTION

Temporal and tissue-specific gene expression depends on *cis*-regulatory elements (CREs) and associated *trans*-acting factors.

In contrast to protein-coding genes, our understanding of *cis*-regulatory DNA is very limited. Analyses of the human epigenome have revealed more than one million DNase I hypersensitive sites (DHS), many of which act as transcriptional enhancers (Thurman et al., 2012); however, the regulatory composition of the vast majority of these elements remain unknown, largely due to the limitations of the technologies previously employed to study CREs.

*Cis*-regulatory DNA is bound and interpreted by protein and RNA complexes and is organized as a 3D structure through long-range chromatin interactions. Identifying the complete composition of a specific CRE *in situ* can provide unprecedented insight into the mechanisms regulating its activity. However, purifying a small chromatin segment from the cellular milieu represents a major challenge—the protein complexes isolated with the targeted chromatin constitute only a small fraction of the co-purified proteins, most of which are non-specific associations. As such, major challenges have limited the application of existing approaches in purifying a specific genomic locus. Chromatin immunoprecipitation (ChIP) assays have provided crucial insights into the genome-wide distribution of TFs and histone marks, but it relies on *a priori* identification of molecular targets and is confined to examining single TFs. Targeted purification of genomic loci with engineered binding sites has been employed to identify single locus-associated proteins, yet it requires knockin gene targeting, which remains inefficient. DNA sequence-specific molecules such as locked nucleic acids (LNAs) (Déjardin and Kingston, 2009) and transcription activator-like (TAL) proteins (Fujita et al., 2013) have been used to enrich large chromatin structures, but these approaches do not enrich for a single genomic locus and cannot be adapted for multiplexed applications. The development of the CRISPR system containing an inactive Cas9 nuclease facilitated sequence-specific enrichment of native genomic regions (Fujita and Fujii, 2013; Waldrip et al., 2014);

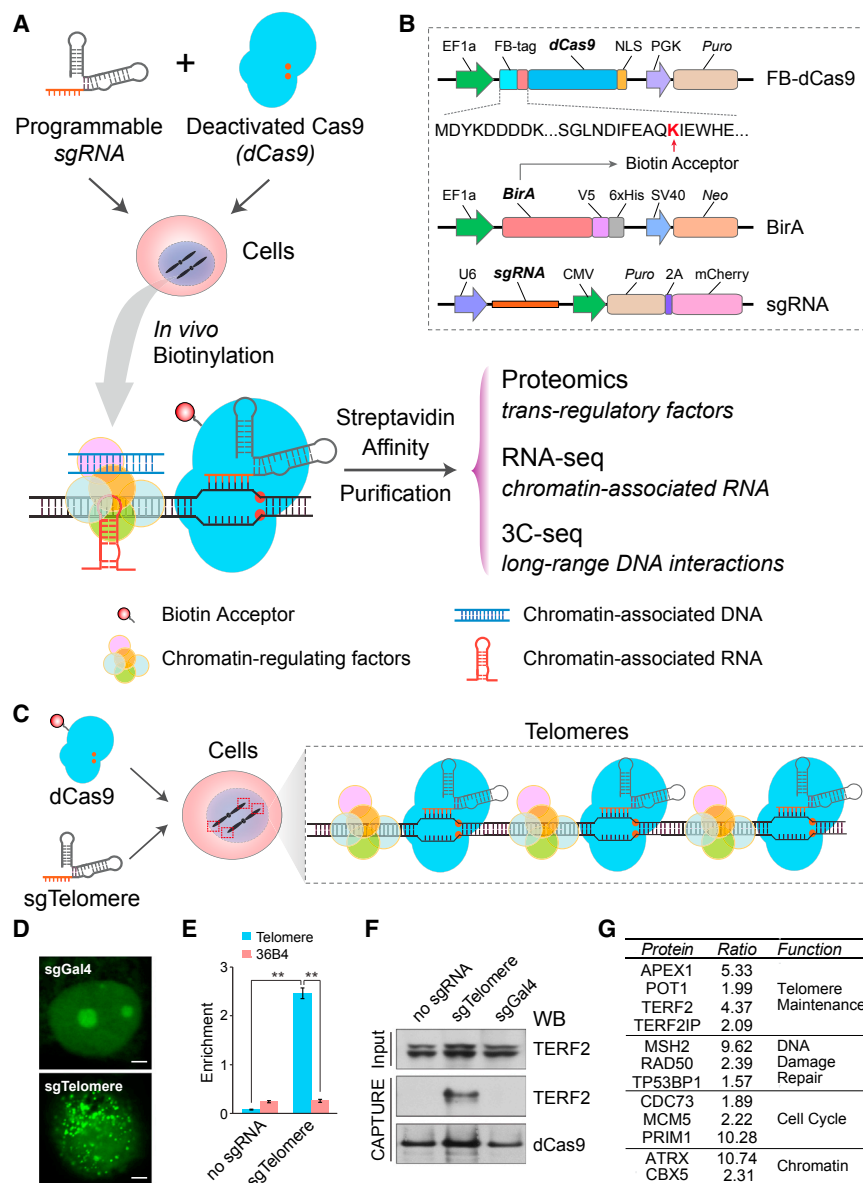


**Figure 1. *In Situ* Capture of Locus-Specific Chromatin Interactions by Biotinylated dCas9**

(A) Schematic of dCas9-mediated capture of chromatin interactions.

(B) The three components of the CAPTURE system: a FB-dCas9, a biotin ligase BirA, and target-specific sgRNAs.

(C) Schematic of dCas9-mediated capture of human telomeres.

(D) Labeling of human telomeres in MCF7 cells. Scale bar, 5  $\mu$ m.

(E) qPCR analysis shows significant enrichment of telomere DNA. Results are mean  $\pm$  SEM of three experiments and analyzed by two-tailed t test. \*\* $p < 0.01$ .

(F) Western blot shows enrichment of TERF2 in sgTelomere-expressing but not control K562 cells with dCas9 alone (no sgRNA) or the non-targeting sgGal4.

(G) iTRAQ-based proteomic analysis of telomere-associated proteins. Representative proteins and the mean iTRAQ ratios are shown. See also Table S3.

ture has the potential to uncover the causal relationship between organizational structure and transcriptional function in a mammalian genome.

## RESULTS

### *In Situ* Capture of Chromatin Interactions by dCas9-Mediated Affinity Purification

To facilitate the analysis of native CREs, we developed a method to isolate chromatin interactions *in situ* (Figure 1A). The core components of CRISPR include Cas9 and a single guide RNA (sgRNA), which serves to direct Cas9 to a target genomic sequence (Cong et al., 2013; Mali et al., 2013). We engineered an N-terminal FLAG and biotin-acceptor-site (FB)-tagged deactivated Cas9 (dCas9) (Figure 1B). Upon *in vivo* biotinylation of dCas9 by the biotin ligase BirA together with sequence-specific sgRNAs in mammalian cells, the genomic locus-associated macromolecules are isolated by high-affinity streptavidin purification. The purified protein, RNA, and DNA complexes are identified and analyzed by mass spectrometry (MS)-based proteomics and high-throughput sequencing for study of native CRE-regulating proteins, RNA, and long-range DNA interactions, respectively (Figure 1A).

This approach has several advantages:

- (1) High sensitivity—the affinity between biotin and streptavidin with  $K_d = 10^{-14}$  mol/L is >1,000-fold higher than antibody-mediated interactions (Kim et al., 2009a; Schatz,

however, these studies were limited to antibody-based purification, whereas the genome-scale specificity and the utility in identifying the *cis*- and *trans*-regulatory components were not evaluated.

Here, we developed an approach to isolate CRE-regulating proteins and long-range DNA interactions by repurposing the CRISPR/Cas9 system. Using human telomeres,  $\beta$ -globin cluster, and embryonic stem cell (ESC) super-enhancers (SEs), we identified *trans*-acting proteins at a single genomic locus. By combining dCas9 capture with chromatin interaction assays, we revealed locus-specific DNA interactions critical for regulatory function. *In situ* capture of SE constituents and disease-associated *cis*-elements provides insight into composition-based hierarchical regulation. Hence, the unbiased analysis of CRE-regulating proteome and 3D interactome by *in situ* cap-

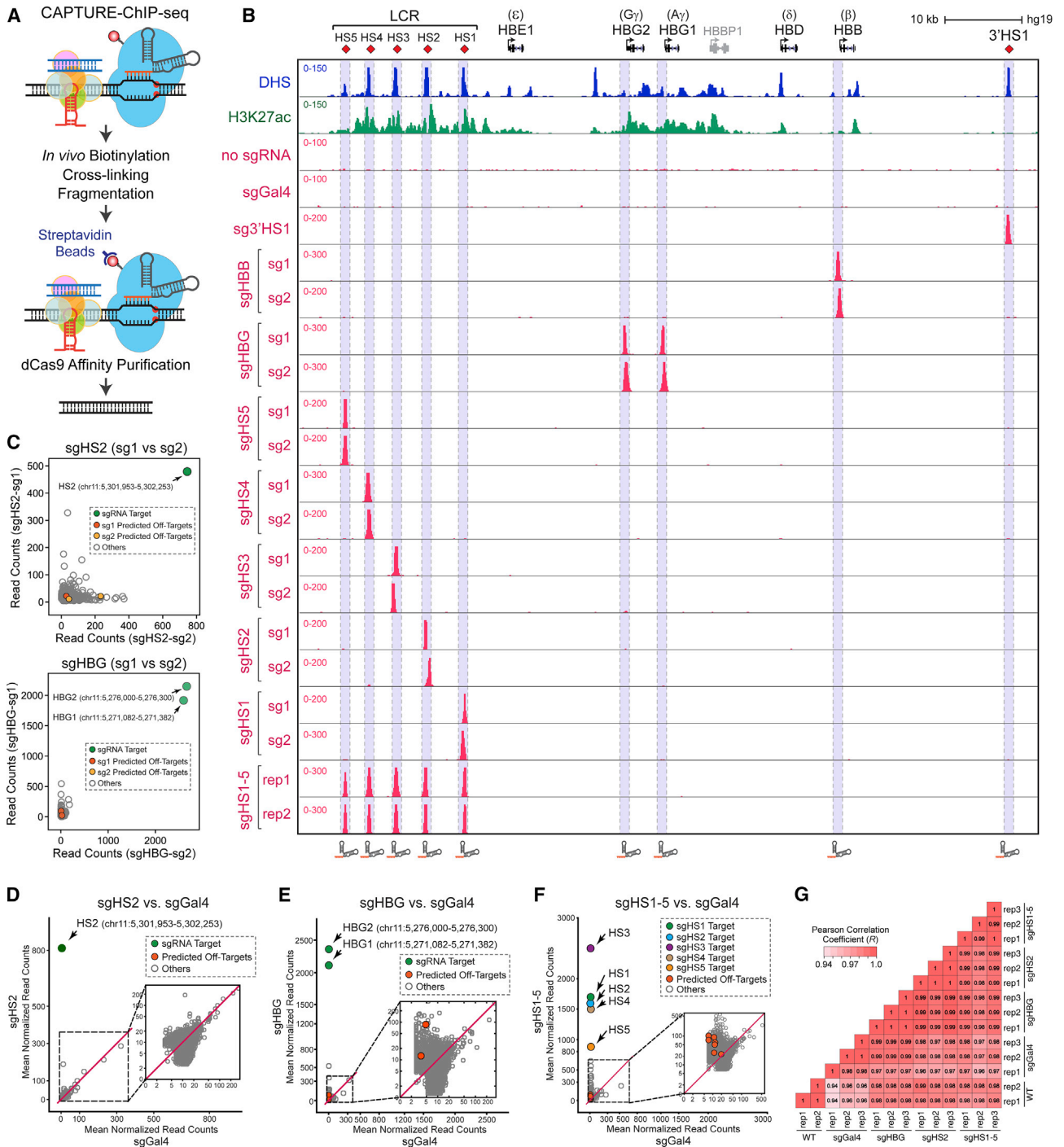


**Figure 2. Biotinylated dCas9-Mediated Capture of the β-Globin Cluster**

(A) Schematic of CAPTURE-ChIP-seq.

(B) Density maps are shown for CAPTURE-ChIP-seq at the β-globin cluster (chr11:5,222,500–5,323,700; hg19) in K562 cells, together with DHS and H3K27ac ChIP-seq profiles. Two independent sgRNAs (sg1 and sg2) or replicate experiments (rep1 and rep2) are shown. Cells expressing dCas9 only (no sgRNA) or dCas9 with sgGal4 were analyzed as controls.

(C) Genome-wide analysis of dCas9 binding in cells expressing two sgRNAs (sg1 and sg2) for HS2 or HBG. Data points for the sgRNA target regions and the predicted off targets are shown as green, red, and orange, respectively. The x and y axis denote the mean normalized read counts from N = 2 to 5 CAPTURE-ChIP-seq experiments.

(legend continued on next page)



1993), thus allowing for more efficient and stable capture of protein-DNA complexes.

- (2) High specificity—this approach avoids using antibodies, which significantly reduces non-specific binding. In addition, the extraordinary stability of biotin-streptavidin allows for stringent purification to eliminate protein contamination.
- (3) Adaptability for multiplexed approaches—the dCas9/sgRNA system can be manipulated by altering sgRNA sequences or combinations, thus allowing for medium- to high-throughput analysis of chromatin interactions.

Taken together, this new approach, which we named CAPTURE (CRISPR affinity purification *in situ* of regulatory elements), has the potential to expedite the analysis of chromatin-templated events by characterizing the entire set of interacting macromolecules and how composition changes during cellular differentiation.

### **In Situ CAPTURE of Human Telomeres**

As a proof-of-principle, we used CAPTURE to isolate human telomeres in K562 cells (Figure 1C). We employed a validated telomere-targeting sgRNA (sgTelomere; Figure 1C) (Chen et al., 2013), which displayed specific labeling of telomeres by the dCas9-EGFP fusion protein, in contrast to the diffuse nuclear localization of the non-targeting dCas9-EGFP (Figure 1D). Upon stable co-expression of sgTelomere and biotinylated dCas9, we observed significant enrichment of telomeric DNA (Figure 1E). The known telomere-associated protein TERF2 was highly enriched in sgTelomere-expressing samples but not in control samples expressing dCas9 alone (no sgRNA) or the non-targeting sgGal4 (Figure 1F). Most importantly, by iTRAQ-based proteomics, we identified many known telomere maintenance proteins (Déjardin and Kingston, 2009; Lewis and Wuttke, 2012) and new telomere-associated proteins (Figure 1G; Table S3).

### **In Situ CAPTURE of $\beta$ -Globin Cluster**

To validate the CAPTURE approach for identifying single copy CREs, we focused on the human  $\beta$ -globin cluster containing five  $\beta$ -like globin genes controlled by a shared enhancer cluster (locus control region [LCR]) with five discrete DHS (HS1–HS5). We designed two or three independent sgRNAs for each promoter (*HBG1*, *HBG2*, and *HBB*), enhancer (HS1–HS4), or insulator (HS5) (Tables S1 and S2). Upon co-expression of sgRNAs and dCas9, K562 chromatin was cross-linked and purified, followed by sequencing of the captured DNA (CAPTURE-ChIP-seq; Figure 2A). We observed specific and significant enrichment of discrete sgRNA-targeted regions (Figure 2B). For example, expression of two sgRNAs for HS1 (sgHS1-sg1 and sg2) led to significant enrichment of HS1 but no other enhancers. Because

of the sequence similarity between *HBG1* and *HBG2*, the sgRNAs targeting *HBG* promoters (sgHBG-sg1 and sg2) do not distinguish the two genes. Consistently, co-expression of sgHBG and dCas9 resulted in significant enrichment of both *HBG* genes. In contrast, binding of dCas9 to  $\beta$ -globin cluster was undetectable when expressed alone (no sgRNA) or with the non-targeting sgGal4. Importantly, co-expression of five sgRNAs (sgHS1–5) led to simultaneous capture of all five LCR enhancers, demonstrating that the CAPTURE system can be adapted for multiplexed analysis of independent CREs. Furthermore, by comparing ChIP-seq intensity using two or three independent sgRNAs, we observed highly specific enrichment of each captured region with minimal off targets (Figures 2C and S1D). Given the consistent performance, hereafter we focus on one sgRNA (sg1; Table S2) for each region unless otherwise specified.

### **Genome-wide Enrichment and Specificity of CAPTURE**

To identify locus-specific interactions, it is critical to evaluate the on-target enrichment and off-target effects. We first compared CAPTURE-ChIP-seq with dCas9 or FLAG antibody-based ChIP-seq using sgHS2 and sgHBG, and we observed significantly higher binding intensity by CAPTURE-ChIP-seq (Figure S1A; Table S1). Among the top 100 peaks by sgHS2, CAPTURE-ChIP-seq led to 18- or 284-fold on-target enrichment compared to dCas9 or FLAG-based ChIP-seq, respectively (Figure S1B). At the global scale, CAPTURE-ChIP-seq resulted in highly specific enrichment of HS2 or *HBG* with many fewer off targets than antibody-based ChIP-seq (Figure S1C). These results provide evidence that the CAPTURE approach allows for more efficient purification of targeted chromatin through improved on-target enrichment and elimination of potential off targets.

We next assessed the genome-wide specificity by comparing dCas9 binding in cells expressing target-specific sgRNAs or sgGal4. Specifically, recruitment of dCas9 by sgHS2 resulted in highly specific enrichment of HS2 with no additional significant dCas9 binding (Figure 2D). Similarly, recruitment of dCas9 by sgHBG led to specific enrichment of *HBG1* and *HBG2*, whereas none of the predicted off targets were significantly enriched (Figure 2E). Moreover, multiplexed capture by sgHS1–5 resulted in identification of LCR enhancers as the top enriched binding sites (Figure 2F). Similar results were obtained with 12 other sgRNAs (Figures S1D and S1E; Table S1). RNA-seq in target-specific sgRNAs, sgGal4, and wild-type (WT) K562 cells revealed minimal transcriptomic changes (Figures 2G and S1F). The expression of  $\beta$ -globin mRNAs remained unchanged (Figure S1G), suggesting that the dCas9 capture did not interfere with the expression of endogenous genes. Together, these analyses establish that the CAPTURE system is highly specific to target loci and can be used to isolate locus-specific regulatory components.

(D–F) Genome-wide differential analysis of dCas9 binding in cells expressing sgHS2, sgHBG, or sgHS1–5 versus sgGal4. Data points for the sgRNA target regions and the predicted off targets are shown as green and red, respectively. N = 5, 4, 6, and 4 CAPTURE-ChIP-seq experiments for sgHS2, sgHBG, sgHS1–5 and sgGal4, respectively.

(G) RNA-seq analysis was performed in cells expressing dCas9 with sgHS2, sgHBG, sgHS1–5, sgGal4, or WT K562 cells. The Pearson correlation coefficient (R) value is shown.

See also Figure S1 and Tables S1 and S2.

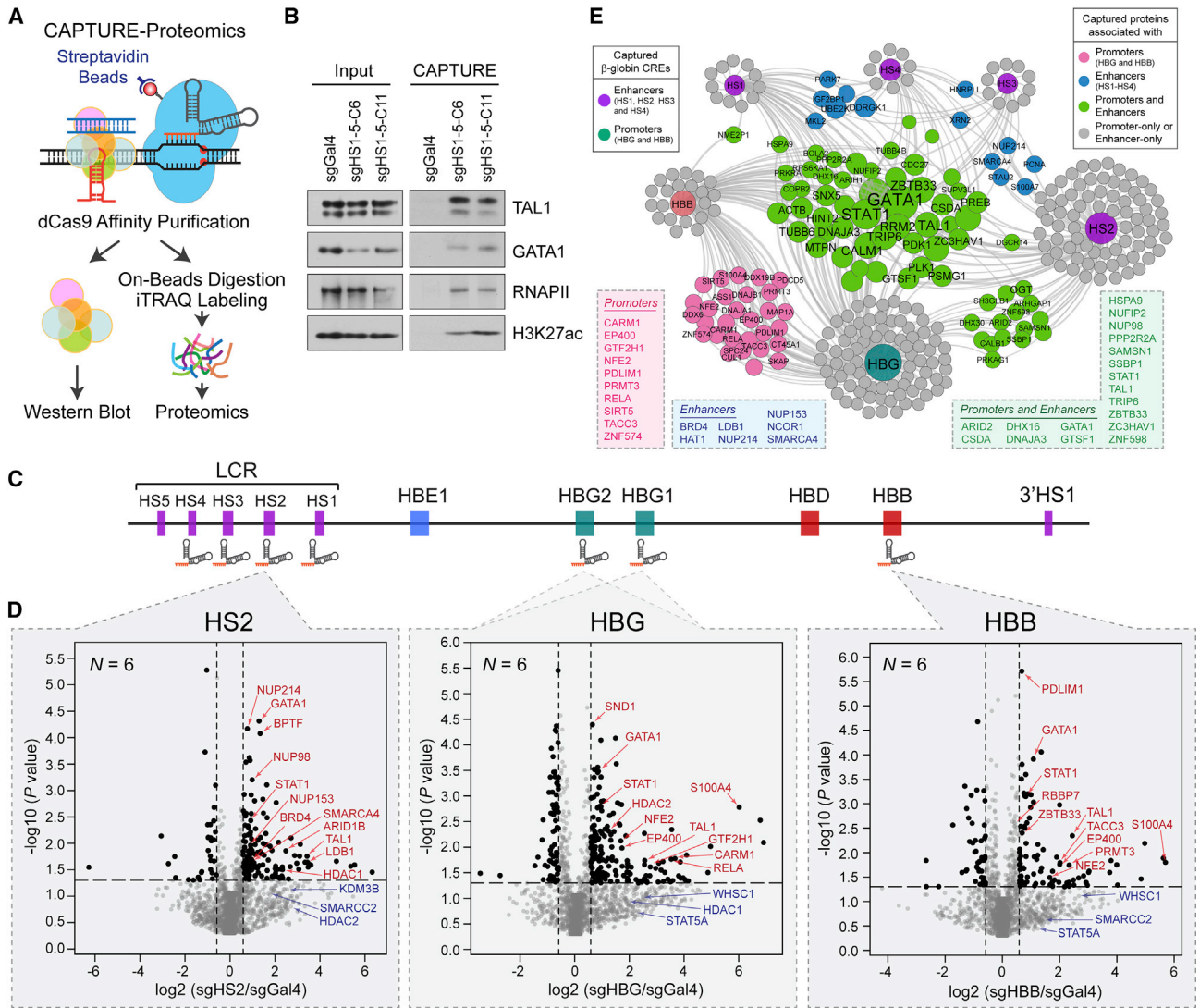


**Figure 3. CAPTURE-Proteomics Identify  $\beta$ -Globin CRE-Associated Protein Complexes**

(A) Schematic of CAPTURE-Proteomics.

(B) Western blot analysis of captured proteins in sgHS1-5 or sgGal4-expressing K562 cells.

(C) Schematic of the  $\beta$ -globin cluster and sgRNAs used for CAPTURE-Proteomics.

(D) CAPTURE-Proteomics identified  $\beta$ -globin CRE-associated proteins. Volcano plots are shown for the iTRAQ proteomics of purifications in sgHS2, sgHBG, or sgHBB versus sgGal4-expressing cells. Relative protein levels in target-specific sgRNAs versus sgGal4 are plotted on the x axis as mean  $\log_2$  iTRAQ ratios across  $N$  replicate experiments. Negative  $\log_{10}$  transformed  $P$  values are plotted on the y axis. Significantly enriched proteins ( $p \leq 0.05$ , iTRAQ ratio  $\geq 1.5$ ) are denoted by black dots, all others by gray dots. Dotted lines indicate 1.5-fold ratio (x axis) and  $P$  value of 0.05 (y axis). Representative chromatin-regulating proteins are denoted by red arrowheads. Representative proteins with iTRAQ ratio  $\geq 1.5$  and  $p > 0.05$  are denoted by blue arrowheads.

(E) Connectivity network of CAPTURE-Proteomics-identified proteins converged by  $\beta$ -globin CREs. The connectivity was built using interactions (gray lines) between proteins and CREs. Colored nodes denote proteins enriched at single or multiple CREs. Size of the circles denotes the frequency of interactions. Inset tables show the lists of representative proteins associated with the  $\beta$ -globin promoters (red), enhancers (blue), or both (green).

See also [Figures S2](#) and [S3](#) and [Table S4](#).

**CAPTURE-Proteomics Identify Trans-acting Regulators of  $\beta$ -Globin Genes**

A major challenge for proteomic analysis of a single genomic locus is the need for a sufficient amount of purified proteins. Hence, we optimized several components of the procedures including protein purification, peptide isolation, and quantitative proteomic profiling, and we developed the “CAPTURE-Prote-

omics” approach to identify locus-specific protein complexes ([Figures 3A](#) and [S2A](#)). We first performed purification in control cell lines to categorize the endogenous biotinylated proteins and/or dCas9-associated non-specific proteins ([Figure S2B](#)). Specifically, we identified proteins purified from K562 cells expressing BirA only, BirA with dCas9, BirA with dCas9 and sgGal4, and BirA with dCas9 and  $\beta$ -globin CRE-specific sgRNAs

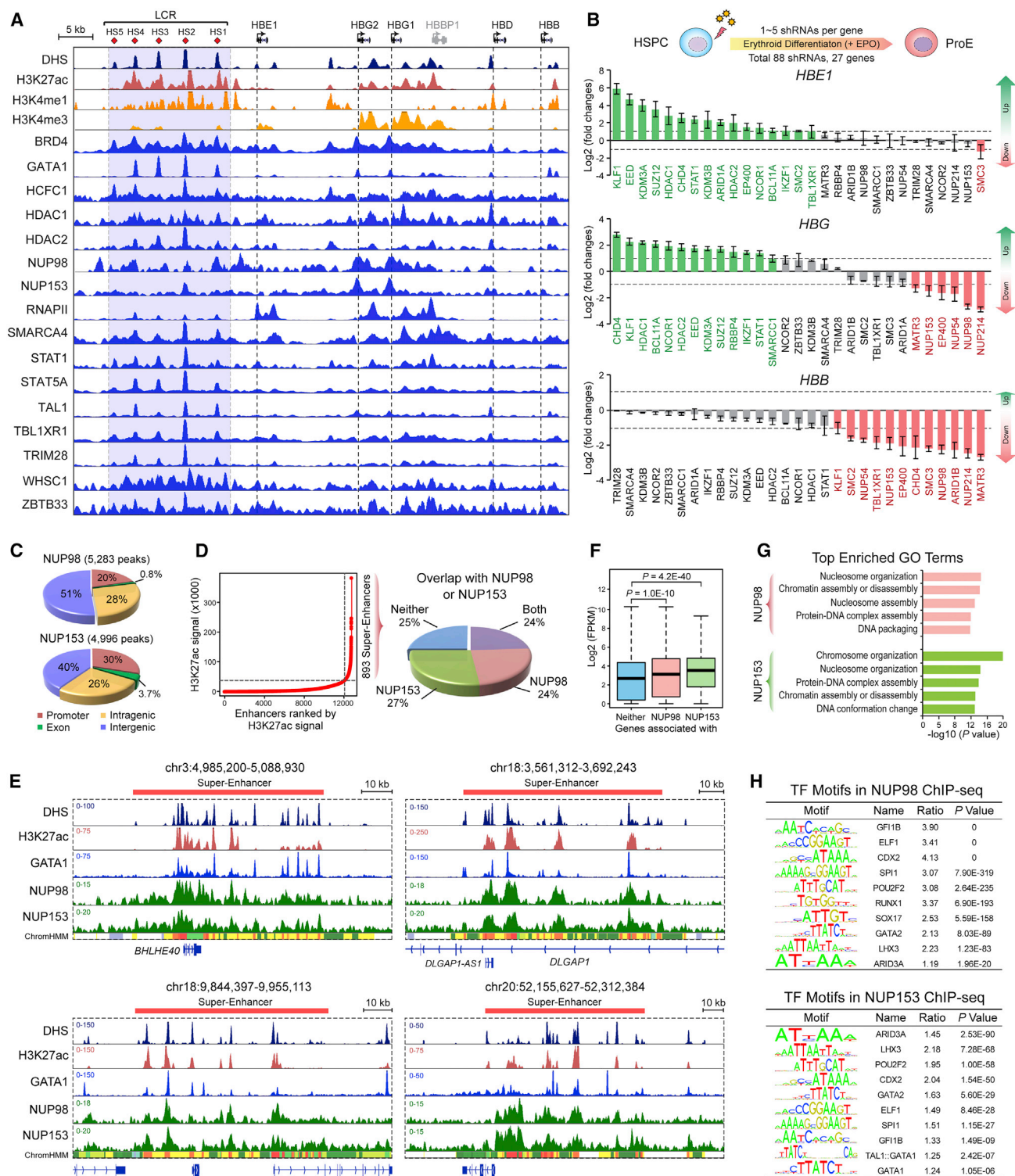


**Figure 4. CAPTURE-Proteomics Identify Known and New Regulators of  $\beta$ -Globin Genes and Erythroid Enhancers**

(A) ChIP-seq analysis of the identified regulators in K562 cells.

(B) RNAi screen of the identified regulators in human primary erythroid cells. Data are plotted as log<sub>2</sub>(fold change) of the  $\beta$ -globin mRNA in each shRNA experiment relative to the non-targeting shNT control. Genes are ranked based on the changes in *HBE1*, *HBG*, or *HBB* expression. shRNAs against *BCL11A* and *KLF1* were analyzed as controls. Results are mean  $\pm$  SEM of all shRNAs for each gene from four experiments.

(legend continued on next page)



in which the endogenous  $\beta$ -globin cluster was deleted (BirA-dCas9-sgAll-Globin-KO; [Method Details](#)). Compiled from three experiments, we identified 304–468 proteins from individual controls, including 277 “high-confidence non-specific proteins” present in all controls ([Figure S2B](#); [Table S4](#)).

We next determined whether known  $\beta$ -globin regulators can be isolated. Co-expression of dCas9 with sgHS1–5 led to significant enrichment of the erythroid TFs (GATA1 and TAL1) required for globin enhancers, together with RNA polymerase II (RNAPII) and acetylated H3K27 (H3K27ac) ([Figure 3B](#)). We then performed iTRAQ-based quantitative proteomics of captured  $\beta$ -globin CREs ([Figure 3C](#)). Relative protein abundance associated with the captured CRE versus sgGal4 was determined by the ratio of the iTRAQ reporter ion intensity. The significance of enrichment ( $P$  value) for each protein was calculated by  $t$  test of the  $\log_2$  iTRAQ ratios in replicate experiments. We surveyed the distribution of high-confidence non-specific proteins in all experiments and observed that 78.3% and 79.8% of them had iTRAQ ratio  $< 1.5$  and  $P$  value  $> 0.05$  ([Figure S2C](#)). Therefore, we employed the iTRAQ ratio  $\geq 1.5$  and  $P$  value  $\leq 0.05$  as the cutoffs and identified 25–164 candidate locus-specific proteins ([Figures 3D](#), [S2D](#), and [S2E](#); [Table S4](#)).

Using CAPTURE-Proteomics, we identified many known factors including GATA1, TAL1, NFE2, components of the SWI/SNF (ARID1A, ARID1B, SMARCA4, and SMARCC1), and NuRD (CHD4, RBBP4, RBBP7, HDAC1, and HDAC2) complexes ([Kim et al., 2009b](#); [Miccio and Blobel, 2010](#); [Xu et al., 2013](#)) at  $\beta$ -globin CREs. More importantly, by locus-specific proteomics, we identified new  $\beta$ -globin CRE-associated complexes including the nucleoporins (NUP98, NUP153, and NUP214), components of the large multiprotein nuclear pore complexes (NPCs), at LCR enhancers ([Figures 3D](#) and [3E](#)). In addition, BRD4 and LDB1 were identified at LCR enhancers, whereas the NuA4 acetyltransferase (EP400) and transcriptional initiation complex (GTF2H1) were found at  $\beta$ -globin promoters. Furthermore, we observed that the *HBG* and *HBB* promoters shared many interacting proteins and clustered closely in protein–DNA connectivity networks ([Figure 3E](#), [S3A](#), and [S3B](#)). By contrast, the distal enhancers (HS1, HS3, and HS4) clustered together to form a distinct subdomain through enhancer-associated proteins, whereas HS2 shared interacting proteins with both subdomains. These analyses provide initial evidence for the composition-based hierarchical organization of the  $\beta$ -globin CREs.

### Identification of New Regulators of $\beta$ -Globin Genes and Erythroid Enhancers

We validated the binding of a subset of the identified proteins in K562 cells by ChIP-seq ([Figure 4A](#); [Table S1](#)). Importantly,

among the factors not previously implicated in  $\beta$ -globin regulation, we confirmed the nucleoporins (NUP98 and NUP153), STAT proteins (STAT1 and STAT5A), TBL1XR1, HCFC1, TRIM28/KAP1, WHSC1/NSD2, and ZBTB33/KAISO to be significantly enriched at one or multiple LCR enhancers by CAPTURE-Proteomics and ChIP-seq. To establish the functional roles, we performed RNAi-mediated loss-of-function analysis in human primary erythroid cells ([Figures 4B](#), [S3G](#), and [S3H](#); [Table S2](#)). Specifically, depletion of 17 of 27 factors led to significant upregulation or downregulation of *HBG* ( $\geq 2$ -fold; [Figure 4B](#)). Similarly, depletion of 15 or 11 of 27 factors led to significant changes in *HBB* or *HBE1* ( $\geq 2$ -fold), respectively. Notably, depletion of NUP98, NUP153, and NUP214 led to marked downregulation of *HBG* (2.8- to 7.3-fold) and *HBB* (3.3- to 5.6-fold), suggesting that the NUP proteins are directly or indirectly required for the activation of  $\beta$ -globin genes.

The peripheral NUPs, including NUP98, NUP153, and NUP214, extend from the membrane-embedded NPC scaffold to regulate nuclear trafficking. While a few NUPs were found to be associated with transcriptionally active genes or regulatory elements ([Capelson et al., 2010](#); [Ibarra et al., 2016](#); [Kalverda et al., 2010](#)), their roles in erythroid enhancers remained unknown. Hence, we performed NUP98 and NUP153 ChIP-seq in K562 cells and identified 5,283 and 4,996 binding sites in gene-proximal promoters and distal elements ([Figure 4C](#)). Notably, NUP98 and NUP153 binding sites are highly enriched at erythroid SEs ([Figures 4D](#) and [4E](#)), associated with gene activation ([Figure 4F](#)), nucleosome organization, and DNA packaging ([Figure 4G](#)), highlighting their potential roles in regulating chromatin organization and/or enhancer activities. Moreover, NUP98/NUP153 binding sites are enriched for motifs associated with hematopoietic TFs, chromatin factors, and homeobox proteins ([Figure 4H](#)), suggesting that NUPs may cooperate with lineage TFs and chromatin regulators in gene transcription. Another identified protein BRD4 binds acetylated histones and plays a critical role in chromatin regulation. Inhibition of BRD4 by a small molecule JQ1 abrogates its function ([Filippakopoulos et al., 2010](#)). BRD4 and related BET proteins (BRD2 and BRD3) are required for globin gene transcription in mouse erythroid cells ([Stonestrom et al., 2015](#)). Consistently, inhibition of BET proteins by JQ1 in human erythroid cells significantly decreased  $\beta$ -globin mRNAs and BRD4 occupancy without apparent effects on erythroid differentiation ([Figures S3C–S3F](#)). Together, these results not only establish new regulators of  $\beta$ -globin enhancers but demonstrate the potential of the CAPTURE approach for unambiguous identification of protein complexes specifically associated with a single genomic locus, such as an enhancer, *in situ*.

(C) Genome-wide distribution of NUP98 and NUP153 ChIP-seq peaks in promoters (–2 kb–1 kb of TSS), exons, intragenic and intergenic regions.

(D) NUP98 and NUP153 associate with erythroid SEs. SEs were identified by ROSE ([Whyte et al., 2013](#)) using the H3K27ac ChIP-seq signal.

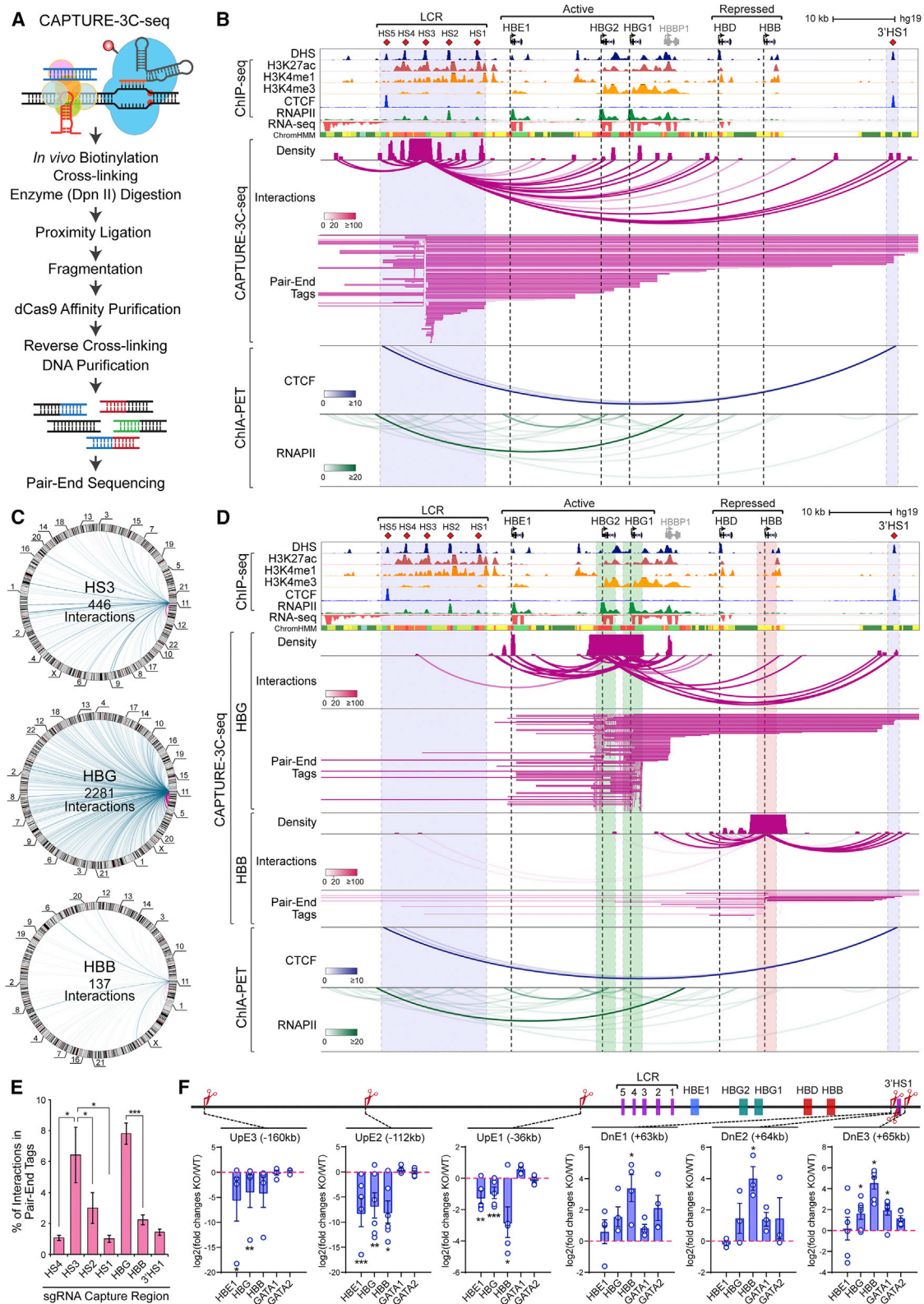
(E) Representative SE loci co-occupied by NUP98 and NUP153. DHS, ChIP-seq, and chromatin state (ChromHMM) data are shown. Red bars denote the annotated SEs.

(F) NUP98- and NUP153-associated genes show significantly higher mRNA expression. Boxes show median of the data and quartiles, and whiskers extend to  $1.5 \times$  of the interquartile range.  $P$  values were calculated by a two-side  $t$  test.

(G) Enriched gene ontology (GO) terms associated with NUP98- or NUP153-occupied regions.

(H) Motif analysis of NUP98 or NUP153 binding sites.





(legend on next page)

### Capture of Long-Range DNA Interactions by Biotinylated dCas9

Enhancers regulate designated promoters over distances by long-range DNA interactions, or chromatin loops. Long-range chromatin interactions have been observed by chromosome conformation capture (3C) (Dekker et al., 2002) and derivative methods including 4C (Simonis et al., 2006; Zhao et al., 2006), 5C (Dostie et al., 2006), and Hi-C (Lieberman-Aiden et al., 2009), as well as fluorescence *in situ* hybridization (FISH) (Osborne et al., 2004). However, these methods are either limited to pre-defined chromatin domains or of low resolution and lacking functional details. For large-scale, *de novo* analysis of chromatin interactions, the ChIA-PET (chromatin interaction analysis by paired-end tag sequencing) approach has been developed (Fullwood et al., 2009; Li et al., 2012). While this method provides unprecedented insight into the principles of 3D genomic architectures, the reliance on specific target proteins and antibodies limits its application in studying a single genomic locus.

To overcome these limitations, we sought to combine chromatin interaction assays with the high-affinity dCas9 capture to unbiasedly identify single genomic locus-associated long-range interactions (CAPTURE-3C-seq; Figure 5A). Specifically, upon co-expression of dCas9 and sgRNAs, long-range chromatin interactions were cross-linked, followed by DpnII digestion and proximity ligation of distant DNA fragments. After fragmentation, locus-specific interactions were captured by dCas9 and analyzed by pair-end sequencing to identify the tethered long-range interactions. Of note, this approach does not involve any pre-selection steps such as PCR-based amplification (Simonis et al., 2006; Zhao et al., 2006) or oligonucleotide-based capture (Hughes et al., 2014), and all interactions brought together by dCas9-tethered DNA were captured in a single experiment.

### CAPTURE-3C-Seq of Locus-Specific DNA Interactions at $\beta$ -Globin Cluster

Using this approach, we first identified long-range interactions at  $\beta$ -globin LCR by targeting dCas9 to HS3 (Figures 5B and 5C; Table S1). From 6,074 pair-end tags (PETs), we identified 446 long-range interactions, including 232 (52.0%) intra-chromosomal interactions, 208 (46.6%) interactions within 1 Mb from HS3, and 126 (28.3%) within the  $\beta$ -globin cluster (Table S5). To quantitatively analyze interactions, we employed the FDR-controlled Bayes factor (BF) to identify “high-confidence interactions” (Figures S4A and S4B; Method Details). Notably, the interaction frequencies were significantly higher between HS3 and

the active genes (*HBG1* and *HBG2*) than the repressed gene (*HBB*), suggesting that the enhancer-promoter loop formation correlates with transcriptional activities. By comparing with CTCF and RNAPII ChIA-PET data (Consortium, 2012; Li et al., 2012), we identified CTCF- or RNAPII-mediated interactions and many new interactions (Figure 5B). By comparing the normalized number and frequency of interactions captured by CAPTURE-3C-seq, ChIA-PET, and Hi-C, we observed that CAPTURE-3C-seq displayed the highest percentage of unique PETs and on-target enrichment (Figure S4C). Compared to 4C-based approach (Schwartzman et al., 2016), CAPTURE-3C-seq displayed a higher percentage of unique PETs but comparable or slightly lower on-target enrichment (Figure S4C).

We then compared the long-range interactions at the active (*HBG*) and repressed (*HBB*) genes (Figure 5D). CAPTURE-3C-seq of *HBG* revealed 215 long-range interactions connecting with most of the  $\beta$ -globin CREs including HS3, *HBE1*, and 3'HS1. Notably, 164 of 215 (76.3%) interactions were between the active *HBG* and *HBE1* genes, whereas no interactions were detected between *HBG* and the repressed *HBB* or *HBD* gene, suggesting that the active genes are interconnected and coregulated through long-range DNA interactions. By contrast, the interactions at *HBB* were predominantly with the proximal *HBD* and 3'HS1.

In CAPTURE-3C-seq, it is critical to rule out that the difference in the position of sgRNA target sites may cause variations in capture efficiency. Therefore, we designed sgRNAs with varying distance to the DpnII site at HS2 or HS3 enhancer (Figure S5A). Importantly, sgRNAs at various positions consistently showed higher frequency of DNA interactions at HS3 than the neighboring HS2 enhancer (Figure S5B). Finally, we compared the interactions captured at discrete  $\beta$ -globin CREs and identified a high-resolution, locus-specific interaction map (Table S5; Figures 5E and S6). While some interactions were shared, most were specific to individual elements. Of note, while HS2, HS3, and HS4 are all required for  $\beta$ -globin gene activation (Fraser et al., 1993; Morley et al., 1992; Navas et al., 1998), HS2 and HS4 contained many fewer interactions than HS3 (Figure 5E, S5, and S6), suggesting that they may cooperate through distinct regulatory composition.

### Identification of *De Novo* CREs for $\beta$ -Globin Genes

Through unbiased capture of HS3, we identified several *de novo* CREs with unknown roles in globin gene regulation (Figures 5F and S7A). By CRISPR-mediated knockout (KO) using paired

#### Figure 5. CAPTURE-3C-Seq Identifies Locus-Specific Long-Range DNA Interactions

(A) Schematic of CAPTURE-3C-seq.

(B) Browser view of the long-range interactions at HS3 (chr11:5,222,500–5,323,700; hg19) is shown. Contact profiles including the density map, interactions (or loops), and PETs are shown. The statistical significance of interactions was determined by the Bayes factor (BF) and indicated by the color scale bars. ChIA-PET, DHS, ChIP-seq, RNA-seq, and ChromHMM data are shown.

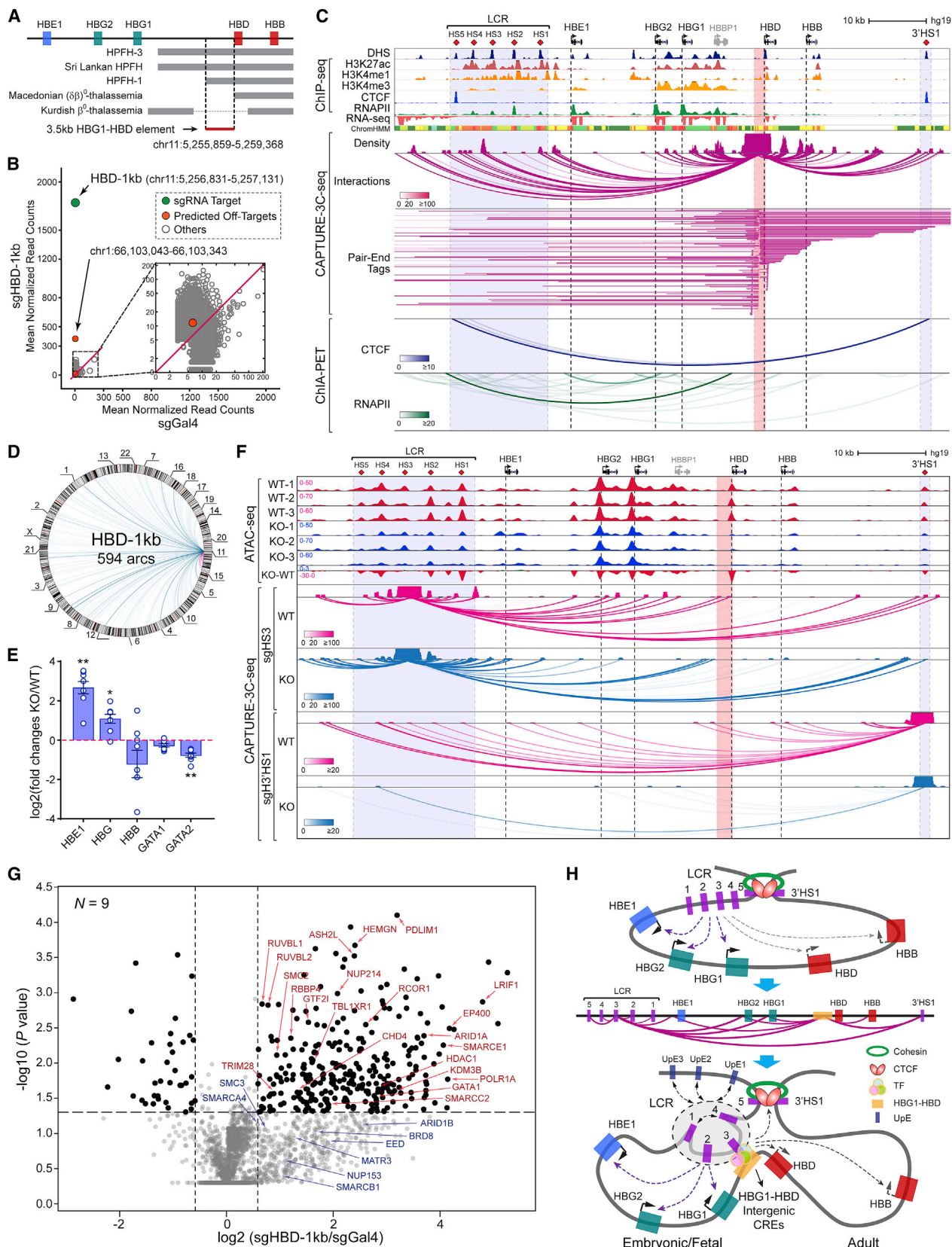
(C) Circlet plots of the long-range interactions are shown. The numbers of identified inter- (blue lines) and intrachromosomal (purple lines) interactions are shown.

(D) Browser view of the long-range interactions at the active *HBG* (green shaded lines) and the repressed *HBB* promoters (red shaded lines) is shown.

(E) The fraction of identified interactions relative to the total PETs at each captured region is shown. Results are mean  $\pm$  SEM of two or three experiments and analyzed by a two-sided t test. \* $p < 0.05$ , \*\*\* $p < 0.001$ .

(F) KO of *de novo* CREs impaired the expression of  $\beta$ -globin genes. The log<sub>2</sub>(fold change) of the mRNA expression in KO versus WT cells are shown. Each circle denotes an independent single-cell-derived KO clone. A diagram depicting the upstream (UpE1, UpE2, and UpE3) and downstream (DnE1, DnE2, and DnE3) CREs is shown on the top. Results are mean  $\pm$  SEM of independent clones and analyzed by a two-sided t test. \* $p < 0.05$ , \*\* $p < 0.01$ , \*\*\* $p < 0.001$ .

See also Figures S4, S5, and S6, and Table S5.



(legend on next page)



sgRNAs, we observed that deletion of the UpE3 element located 160 kb upstream of *HBE1* led to significant downregulation of  $\beta$ -globin mRNAs (Figure 5F). Similarly, KO of UpE2 (–112 kb) and UpE1 (–36 kb) resulted in significant downregulation of  $\beta$ -globin genes. By contrast, KO of three downstream elements (DnE1, DnE2, and DnE3) overlapping with the CTCF-associated insulator resulted in significant upregulation of the repressed *HBB* gene, whereas the expression of *HBE1*, *HBG*, *GATA1*, and *GATA2* remained largely unaffected. The identification of new  $\beta$ -globin CREs illustrates the presence of additional distal *cis*-elements not recapitulated in studies using mouse models (Hardison et al., 1997; Navas et al., 1998; Peterson et al., 1998).

### In Situ CAPTURE of a Disease-Associated CRE

Disease-associated CREs are commonly recognized by correlative chromatin features, yet limited insight has been gained into their regulatory composition. One example is the 3.5 kb *HBG1-HBD* intergenic region required for the silencing of fetal  $\beta$ -globin genes (Figure 6A). Genetic mapping studies showed that deletion of this region in humans, including in hereditary persistence of fetal hemoglobin 1 (HPFH-1), HPFH-3, and Sri Lankan HPFH patients, led to reactivation of *HBG*. By contrast, in patients that retained the intergenic region, including Macedonian ( $\delta\beta^0$ -thalassemia and Kurdish  $\beta^0$ -thalassemia, *HBG* silencing was maintained (Sankaran et al., 2011). While these studies established the *HBG1-HBD* intergenic region as a critical disease-associated CRE, the underlying regulatory components remained unclear.

Therefore, we designed three sgRNAs targeting the 3.5 kb *HBG1-HBD* intergenic element (HBD-1kb, HBD-1.5kb and HBD-2kb; Figure S7B). The specificity of the sgRNAs was confirmed by CAPTURE-ChIP-seq (Figure 6B). By CAPTURE-3C-seq, we observed that the HBD-1kb region contained significantly higher frequency of long-range interactions than the neighboring HBD-1.5kb and HBD-2kb regions (Figure S7B). These interactions connected HBD-1kb with most  $\beta$ -globin CREs, including the HS1–HS4 enhancers,  $\beta$ -globin genes, and insulators (Figures 6C and 6D). Notably, KO of HBD-1kb in K562 cells resulted in upregulation of *HBE1* and *HBG*, whereas *HBB* was largely unaffected (Figure 6E). HBD-1kb KO also led to marked decreases in chromatin accessibility at the *HBG* and *HBD* promoters; HS1, HS2, and HS4 enhancers; and

3'HS1 (Figure 6F). Furthermore, by CAPTURE-3C-seq, we observed significant changes in the frequency of long-range interactions at several CREs (Figure 6F), suggesting that the *HBG1-HBD* intergenic region is required for the proper chromatin configuration and the expression of  $\beta$ -globin genes.

By CAPTURE-Proteomics of the *HBG1-HBD* intergenic region, we identified components of the SWI/SNF and NuRD complexes, transcriptional co-activators (EP400, KDM3B, and ASH2L), co-repressors (RCOR1, TBL1XR1, LRIF1, and TRIM28/KAP1), cohesin (SMC3), nucleoporins (NUP153 and NUP214) and TFs (GATA1 and STAT1) (Figure 6G; Table S4). The identification of the SWI/SNF and cohesin proteins is consistent with their function in regulating chromatin looping (Kagey et al., 2010; Kim et al., 2009b). The presence of co-activators and co-repressors may be related to the interactions with both active and repressed  $\beta$ -globin genes (Figure 6C). Notably, most of the HBD-1kb-associated proteins were not identified at the neighboring HBD-1.5kb or HBD-2kb region (Figure S7C).

Together, our studies support a refined model for the spatial organization of the  $\beta$ -globin CREs (Figure 6H). The  $\beta$ -globin genes are coordinately regulated in an insulated neighborhood between HS5 and 3'HS1. The *HBG1-HBD* intergenic region functions as a major interaction hub linking enhancers and insulators to establish two subdomains: an embryonic/fetal subdomain containing *HBE1*, *HBG1*, and *HBG2* genes and an adult subdomain containing *HBD* and *HBB*. HS2 and other LCR enhancers cooperate with associated regulators to activate the embryonic/fetal or adult genes in a developmental-stage-specific manner. Thus, our in-depth analyses of locus-specific interactions at the  $\beta$ -globin cluster by *in situ* CAPTURE not only reveal new spatial features for the composition-based hierarchical control of a lineage-specific enhancer cluster but also establish new approaches for molecular dissection of disease-associated CREs.

### In Situ CAPTURE of Developmentally Regulated SEs

To demonstrate the utility of CAPTURE across cell models, we analyzed lineage-specific SEs during mouse ESC differentiation. We generated a site-specific knockin allele containing FB-dCas9-EGFP and BirA through FLPe-mediated recombination (Beard et al., 2006) (Figure 7A). After confirming the

### Figure 6. Biotinylated dCas9-Mediated In Situ Capture of a Disease-Associated CRE

- (A) Schematic of the 3.5 kb intergenic element (chr11:5,255,859–5,259,368; hg19) along with the deletions mapped in prior studies.
- (B) Genome-wide specificity of sgHBD-1kb was measured by CAPTURE-ChIP-seq. N = 2 and 4 experiments for sgHBD-1kb and sgGal4.
- (C) Browser view of the long-range interactions at HBD-1kb (red shaded lines) is shown.
- (D) Circlet plot of the long-range interactions at HBD-1kb is shown.
- (E) HBD-1kb KO impaired the expression of  $\beta$ -globin genes. Results are mean  $\pm$  SEM of independent KO clones and analyzed by a two-sided t test. \*p < 0.05, \*\*p < 0.01.
- (F) HBD-1kb KO led to altered chromatin accessibility and long-range interactions. Results from three ATAC-seq experiments in WT or KO cells are shown. Regions showing increased or decreased ATAC-seq signals in KO relative to WT cells (KO-WT) are depicted in green and red, respectively. HS3- or 3'HS1-mediated long-range interactions were determined by CAPTURE-3C-seq.
- (G) CAPTURE-Proteomics identified HBD-1kb-associated proteins. Volcano plot is shown for the iTRAQ proteomics of purifications in sgHBD-1kb versus sgGal4-expressing cells.
- (H) The model of composition-based organization of the  $\beta$ -globin cluster. Top: A previously described model depicting an active chromatin hub (ACH) formed through spatial organization of  $\beta$ -globin CREs (Palstra et al., 2003; Tolhuis et al., 2002). Middle: Two-dimensional representation of the long-range DNA interactions (purple lines) identified at HS3 and the *HBG1-HBD* intergenic CREs (yellow square) by CAPTURE. Bottom: A refined model depicting the composition-based spatial and hierarchical organization of the  $\beta$ -globin CREs.
- See also Figure S7 and Tables S4 and S5.



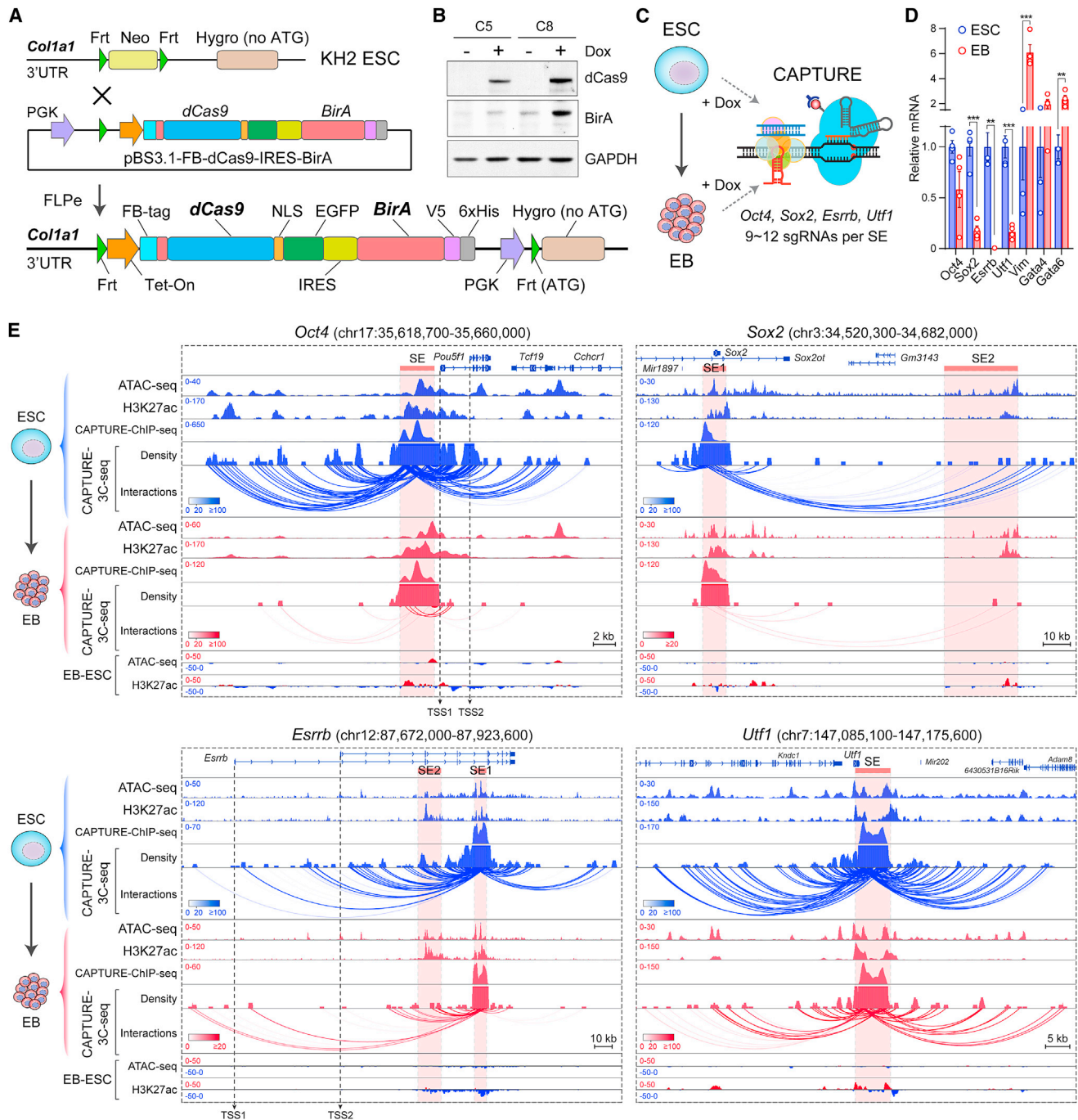


**Figure 7. Multiplexed CAPTURE of Developmentally Regulated SEs during Differentiation**

(A) Schematic of site-specific knockin of tetracycline-inducible FB-dCas9-EGFP and BirA.

(B) Dox-inducible expression of dCas9 and BirA proteins was confirmed by western blot in two independent knockin ESC lines.

(C) Schematic of multiplexed CAPTURE of ESC-specific SEs in ESCs and EBs.

(D) Differentiated EBs were characterized by downregulation of ESC-associated genes (*Oct4*, *Sox2*, *Esrrb*, and *Utf1*) and upregulation of differentiation-associated genes (*Vim*, *Gata4*, and *Gata6*). Results are mean  $\pm$  SEM of 3 or 4 experiments and analyzed by a two-sided t test. \*\* $p < 0.01$ , \*\*\* $p < 0.001$ .

(E) Browser view of SE-associated long-range interactions captured by CAPTURE-3C-seq in ESCs and EBs. Regions showing increased or decreased ATAC-seq or H3K27ac ChIP-seq signals in EBs relative to ESCs (EB-ESC) are depicted in red and blue, respectively. Red bars denote the annotated SEs. Dashed lines denote the alternative TSS of transcript variants for *Oct4* (*Pou5f1*) and *Esrrb*.

doxycycline (Dox)-inducible expression of dCas9 and BirA proteins (Figure 7B), ESCs were differentiated to embryoid bodies (EBs). We designed multiplexed sgRNAs targeting four ESC-specific SEs (*Oct4*, *Sox2*, *Esrrb*, and *Utf1*; Figure 7C). Upon differentiation, the expression of the SE-linked genes was significantly downregulated (Figure 7D). We then analyzed SE-associated long-range interactions and chromatin features (Figure 7E). Strikingly, *in situ* CAPTURE of distinct SEs revealed frequent long-range interactions between SEs and their gene targets in ESCs, whereas the interactions were significantly less or absent in EBs. More importantly, the significant changes in SE-mediated long-range interactions, together with minimal or no changes in chromatin accessibility or H3K27ac, demonstrate that the loss of enhancer-promoter contacts precedes changes in chromatin landscape during differentiation. These findings support a model in which enhancer-promoter loop formation causally underlies gene activation (Deng et al., 2012; Deng et al., 2014). Many long-range interactions were between different SEs (*Sox2* and *Esrrb*; Figure 7E) or between SEs and promoters of transcript variants (*Oct4* and *Esrrb*). Furthermore, while most long-range interactions were absent or weakened in EBs, some were maintained, indicating a dynamic and hierarchical regulation of SE interactions in response to cellular differentiation. Taken together, our studies demonstrate that the CAPTURE approaches work effectively in human cells and transgenic mouse ESCs, raising the prospect of using biotinylated dCas9 in purification of CRE-associated chromatin interactions across cellular conditions *in situ* and in developing tissues *in vivo*.

## DISCUSSION

### *In Situ* CAPTURE of Locus-Specific Interactions

Current technologies in studying chromatin structure rely on 3D genome-mapping approaches. The basic principle is nuclear proximity ligation that allows detection of distant interacting DNA tethered together by higher-order architectures. ChIA-PET was designed to detect genome-wide chromatin interactions mediated by specific protein factors. Hi-C was developed to capture all chromatin contacts, particularly large-scale structures including the topologically associated domains (TADs) (Dixon et al., 2012); however, it lacked the level of resolution required for locus-specific interactions as well as the information of the *trans*-acting factors mediating such interactions. Hence, the CAPTURE method provides a complementary approach for high-resolution, unbiased analysis of locus-specific proteome and 3D interactome that is not dependent on predefined proteins, available reagents, or *a priori* knowledge of the target loci. The CAPTURE approach has several unique features, including the ability to specifically detect macromolecules at an endogenous locus with minimal off targets, to identify combinatorial protein-DNA interactions, and to dissect the disease-associated or developmentally regulated *cis*-elements.

### Important Considerations for *In Situ* CAPTURE

For selective capture of locus-specific chromatin interactions, the following parameters need to be carefully evaluated. First,

the sgRNA target sequences should locate in close proximity to the captured element to maximize the capture efficiency, but not overlap with TF binding sites to avoid interference with protein-DNA interactions. Second, the on-target enrichment and genome-wide specificity by independent sgRNAs should be evaluated to minimize off targets. Third, the study of locus-specific proteome requires the identification of non-specific proteins in control cells for quantitative and statistical analysis. Fourth, the analysis of CRE-mediated long-range DNA interactions requires the design of sgRNAs in close proximity to DpnII sites. Finally, the use of multiplexed sgRNAs targeting multiple CREs at the same enhancer or multiple enhancers helps distinguish consistent interactions from rare interactions of individual sgRNAs; however, the selection of multiplexed sgRNAs requires comparable on-target enrichment for each sgRNA to minimize variation in capture efficiency.

### Multiplexed CAPTURE of SE Composition

Intensively marked clusters of enhancers or SEs have been described, yet the underlying principles of enhancer clustering remained unclear. Here, we focus on an erythroid-specific SE, or LCR, controlling the expression of  $\beta$ -globin genes. The  $\beta$ -globin LCR consists of five DHS, three of which display enhancer activities. Specifically, HS2 behaves as a classical enhancer in reporter assays (Fraser et al., 1993; Morley et al., 1992), whereas the enhancer activities of HS3 and HS4 can only be detected in the context of chromatin (Hardison et al., 1997; Navas et al., 1998). By *in situ* capture of  $\beta$ -globin CREs, our studies uncover distinguishing features in the regulatory composition of SE constituents. Importantly, the *HBG* and *HBB* promoters shared many interacting proteins and clustered closely, whereas the HS1, HS3, and HS4 enhancers clustered to form a distinct subdomain. HS2 shared interacting proteins with both subdomains. Furthermore, HS3 contains significantly more long-range interactions than the nearby enhancers. Hence, our results support a model for the hierarchical organization of the  $\beta$ -globin LCR, in which HS2 functions as a conventional enhancer by providing binding sites for *trans*-acting factors, whereas HS3 mediates long-range chromatin looping. Hence, the SE constituents cooperate through distinct regulatory composition to function within the same SE cluster. These findings also help explain the distinct requirement of HS2 and HS3 for the transgenic versus endogenous  $\beta$ -globin gene expression. Thus, the CAPTURE approach provides a platform for the systematic dissection of SE constituents and the underlying formative composition controlling enhancer structure-function.

Finally, the CAPTURE system can be adapted for multiplexed analysis of multiple CREs at the same enhancer or multiple enhancers, thus allowing for high-throughput capture of locus-specific interactions. High-resolution, multiplexed analysis of chromatin interactions at developmentally regulated enhancers provides evidence for the causality of chromatin looping and enhancer activities. Conversely, unbiased analysis of promoter-associated interactions will help identify the complete set of constitutive or tissue-specific distal CREs, thus allowing for comprehensive analysis of regulatory CREs of any gene. The vast majority of disease-associated variants reside within

non-coding elements and exert effects through long-range regulation of gene expression. The unbiased analysis of chromatin-templated hierarchical events will help define the underlying regulatory principles, thus advancing our mechanistic understanding of the non-coding genome in human disease.

## STAR★METHODS

Detailed methods are provided in the online version of this paper and include the following:

- **KEY RESOURCES TABLE**
- **CONTACT FOR REAGENT AND RESOURCE SHARING**
- **EXPERIMENTAL MODEL AND SUBJECT DETAILS**
  - Cells and Cell Culture
- **METHOD DETAILS**
  - sgRNA Cloning and Transduction
  - CAPTURE-ChIP-seq
  - CAPTURE-Proteomics
  - CAPTURE-3C-seq
  - CRISPR Imaging of Human Telomeres
  - RNA-seq and qRT-PCR Analysis
  - ChIP-seq Analysis
  - ATAC-seq Analysis
  - Flow Cytometry
  - Cytospin
  - CRISPR/Cas9-Mediated Knockout of *Cis*-Regulatory Elements
  - Generation of Tetracycline-Inducible dCas9 Knockin ESCs
- **QUANTIFICATION AND STATISTICAL ANALYSIS**
- **DATA AND SOFTWARE AVAILABILITY**

## SUPPLEMENTAL INFORMATION

Supplemental Information includes seven figures and five tables and can be found with this article online at <http://dx.doi.org/10.1016/j.cell.2017.08.003>.

## AUTHOR CONTRIBUTIONS

Conceptualization: X.L. and J.X.; Methodology: X.L., Y.Z., Y.C., M.L., F.Z., K.L., H.C., M.N., Y.L., Z.G., K.E.D., S.X., G.C.H., Z.X., M.Q.Z., Z.S., and J.X.; Investigation: X.L., F.Z., K.L., H.C., and J.X.; Writing – Original Draft: X.L., Y.Z., Y.C., M.L., and J.X.; Writing – Review & Editing: J.X.; Funding Acquisition: F.Z., M.Q.Z., Z.S., and J.X.; Supervision, Z.X., M.Q.Z., Z.S., and J.X.

## ACKNOWLEDGMENTS

We thank B. Chen and B. Huang at UCSF for the CRISPR imaging reagents and discussion; L. Wang, Y. Du, and D. Trudgian at UTSW BioHPC for assistance; and S.T. Smale at UCLA for critical reading of the manuscript and discussion. This work was supported by the NIH grant R01MH102616, the Cecil H. and Ida Green Endowment, the SKR&DPC grant (2017YFA0505503), and the NSFC grants (91519326, 31671384) to M.Q.Z.; the NSFC grant (31670836), the National Key R&D Program of China (2017YFA0505100), and Shanghai Institute of Higher Learning (TP2015003) to F.Z.; the “100-Talent” Program of Chinese Academy of Sciences (Y516C11851) to Z.S.; the NIH grants K01DK093543, R03DK101665, and R01DK111430, a Cancer Prevention and Research Institute of Texas (CPRIT) New Investigator award (RR140025), the American Cancer Society award and the Harold C. Simmons Comprehensive Cancer Center at UT Southwestern (IRG-02-196), the Welch

Foundation grant I-1942-20170325, and an American Society of Hematology Scholar award to J.X.

Received: October 27, 2016

Revised: May 23, 2017

Accepted: August 1, 2017

Published: August 24, 2017

## REFERENCES

- Beard, C., Hochedlinger, K., Plath, K., Wutz, A., and Jaenisch, R. (2006). Efficient method to generate single-copy transgenic mice by site-specific integration in embryonic stem cells. *Genesis* 44, 23–28.
- Capelson, M., Liang, Y., Schulte, R., Mair, W., Wagner, U., and Hetzer, M.W. (2010). Chromatin-bound nuclear pore components regulate gene expression in higher eukaryotes. *Cell* 140, 372–383.
- Chen, B., Gilbert, L.A., Cimini, B.A., Schnitzbauer, J., Zhang, W., Li, G.W., Park, J., Blackburn, E.H., Weissman, J.S., Qi, L.S., and Huang, B. (2013). Dynamic imaging of genomic loci in living human cells by an optimized CRISPR/Cas system. *Cell* 155, 1479–1491.
- Cong, L., Ran, F.A., Cox, D., Lin, S., Barretto, R., Habib, N., Hsu, P.D., Wu, X., Jiang, W., Marraffini, L.A., and Zhang, F. (2013). Multiplex genome engineering using CRISPR/Cas systems. *Science* 339, 819–823.
- Consortium, T.E.P.; ENCODE Project Consortium (2012). An integrated encyclopedia of DNA elements in the human genome. *Nature* 489, 57–74.
- Déjardin, J., and Kingston, R.E. (2009). Purification of proteins associated with specific genomic loci. *Cell* 136, 175–186.
- Dekker, J., Rippe, K., Dekker, M., and Kleckner, N. (2002). Capturing chromosome conformation. *Science* 295, 1306–1311.
- Deng, W., Lee, J., Wang, H., Miller, J., Reik, A., Gregory, P.D., Dean, A., and Blobel, G.A. (2012). Controlling long-range genomic interactions at a native locus by targeted tethering of a looping factor. *Cell* 149, 1233–1244.
- Deng, W., Rupon, J.W., Krivega, I., Breda, L., Motta, I., Jahn, K.S., Reik, A., Gregory, P.D., Rivella, S., Dean, A., and Blobel, G.A. (2014). Reactivation of developmentally silenced globin genes by forced chromatin looping. *Cell* 158, 849–860.
- Dixon, J.R., Selvaraj, S., Yue, F., Kim, A., Li, Y., Shen, Y., Hu, M., Liu, J.S., and Ren, B. (2012). Topological domains in mammalian genomes identified by analysis of chromatin interactions. *Nature* 485, 376–380.
- Dostie, J., Richmond, T.A., Arnaout, R.A., Selzer, R.R., Lee, W.L., Honan, T.A., Rubio, E.D., Krumm, A., Lamb, J., Nusbaum, C., et al. (2006). Chromosome Conformation Capture Carbon Copy (5C): a massively parallel solution for mapping interactions between genomic elements. *Genome Res.* 16, 1299–1309.
- Elias, J.E., and Gygi, S.P. (2007). Target-decoy search strategy for increased confidence in large-scale protein identifications by mass spectrometry. *Nat. Methods* 4, 207–214.
- Filippakopoulos, P., Qi, J., Picaud, S., Shen, Y., Smith, W.B., Fedorov, O., Morse, E.M., Keates, T., Hickman, T.T., Felletar, I., et al. (2010). Selective inhibition of BET bromodomains. *Nature* 468, 1067–1073.
- Fraser, P., Pruzina, S., Antoniou, M., and Grosveld, F. (1993). Each hypersensitive site of the human beta-globin locus control region confers a different developmental pattern of expression on the globin genes. *Genes Dev.* 7, 106–113.
- Fujita, T., Asano, Y., Ohtsuka, J., Takada, Y., Saito, K., Ohki, R., and Fujii, H. (2013). Identification of telomere-associated molecules by engineered DNA-binding molecule-mediated chromatin immunoprecipitation (enChIP). *Sci. Rep.* 3, 3171.
- Fujita, T., and Fujii, H. (2013). Efficient isolation of specific genomic regions and identification of associated proteins by engineered DNA-binding molecule-mediated chromatin immunoprecipitation (enChIP) using CRISPR. *Biochem. Biophys. Res. Commun.* 439, 132–136.

- Fullwood, M.J., Liu, M.H., Pan, Y.F., Liu, J., Xu, H., Mohamed, Y.B., Orlov, Y.L., Velkov, S., Ho, A., Mei, P.H., et al. (2009). An oestrogen-receptor-alpha-bound human chromatin interactome. *Nature* **462**, 58–64.
- Hardison, R., Slightom, J.L., Gumucio, D.L., Goodman, M., Stojanovic, N., and Miller, W. (1997). Locus control regions of mammalian beta-globin gene clusters: combining phylogenetic analyses and experimental results to gain functional insights. *Gene* **205**, 73–94.
- Huang, J., Liu, X., Li, D., Shao, Z., Cao, H., Zhang, Y., Trompouki, E., Bowman, T.V., Zon, L.I., Yuan, G.C., et al. (2016). Dynamic control of enhancer reporters drives lineage and stage-specific transcription during hematopoiesis. *Dev. Cell* **36**, 9–23.
- Hughes, J.R., Roberts, N., McGowan, S., Hay, D., Giannoulitou, E., Lynch, M., De Gobbi, M., Taylor, S., Gibbons, R., and Higgs, D.R. (2014). Analysis of hundreds of cis-regulatory landscapes at high resolution in a single, high-throughput experiment. *Nat. Genet.* **46**, 205–212.
- Ibarra, A., Benner, C., Tyagi, S., Cool, J., and Hetzer, M.W. (2016). Nucleoporin-mediated regulation of cell identity genes. *Genes Dev.* **30**, 2253–2258.
- Kagey, M.H., Newman, J.J., Bilodeau, S., Zhan, Y., Orlando, D.A., van Berkum, N.L., Ebmeier, C.C., Goossens, J., Rahl, P.B., Levine, S.S., et al. (2010). Mediator and cohesin connect gene expression and chromatin architecture. *Nature* **467**, 430–435.
- Kalverda, B., Pickersgill, H., Shloma, V.V., and Fornerod, M. (2010). Nucleoporins directly stimulate expression of developmental and cell-cycle genes inside the nucleoplasm. *Cell* **140**, 360–371.
- Kass, R.E., and Raftery, A.E. (1995). Bayes Factors. *J. Am. Stat. Assoc.* **90**, 773–795.
- Kim, J., Cantor, A.B., Orkin, S.H., and Wang, J. (2009a). Use of in vivo biotinylation to study protein-protein and protein-DNA interactions in mouse embryonic stem cells. *Nat. Protoc.* **4**, 506–517.
- Kim, S.I., Bultman, S.J., Kiefer, C.M., Dean, A., and Bresnick, E.H. (2009b). BRG1 requirement for long-range interaction of a locus control region with a downstream promoter. *Proc. Natl. Acad. Sci. USA* **106**, 2259–2264.
- Langmead, B., and Salzberg, S.L. (2012). Fast gapped-read alignment with Bowtie 2. *Nat. Methods* **9**, 357–359.
- Langmead, B., Trapnell, C., Pop, M., and Salzberg, S.L. (2009). Ultrafast and memory-efficient alignment of short DNA sequences to the human genome. *Genome Biol.* **10**, R25.
- Lewis, K.A., and Wuttke, D.S. (2012). Telomerase and telomere-associated proteins: structural insights into mechanism and evolution. *Structure* **20**, 28–39.
- Li, G., Ruan, X., Auerbach, R.K., Sandhu, K.S., Zheng, M., Wang, P., Poh, H.M., Goh, Y., Lim, J., Zhang, J., et al. (2012). Extensive promoter-centered chromatin interactions provide a topological basis for transcription regulation. *Cell* **148**, 84–98.
- Lieberman-Aiden, E., van Berkum, N.L., Williams, L., Imakaev, M., Ragoczy, T., Telling, A., Amit, I., Lajoie, B.R., Sabo, P.J., Dorschner, M.O., et al. (2009). Comprehensive mapping of long-range interactions reveals folding principles of the human genome. *Science* **326**, 289–293.
- Ma, W., Ay, F., Lee, C., Gulsoy, G., Deng, X., Cook, S., Hesson, J., Cavanaugh, C., Ware, C.B., Krumm, A., et al. (2015). Fine-scale chromatin interaction maps reveal the cis-regulatory landscape of human lincRNA genes. *Nat. Methods* **12**, 71–78.
- Mali, P., Yang, L., Esvelt, K.M., Aach, J., Guell, M., DiCarlo, J.E., Norville, J.E., and Church, G.M. (2013). RNA-guided human genome engineering via Cas9. *Science* **339**, 823–826.
- McLean, C.Y., Bristor, D., Hiller, M., Clarke, S.L., Schaar, B.T., Lowe, C.B., Wenger, A.M., and Bejerano, G. (2010). GREAT improves functional interpretation of cis-regulatory regions. *Nat. Biotechnol.* **28**, 495–501.
- Miccio, A., and Blobel, G.A. (2010). Role of the GATA-1/FOG-1/NuRD pathway in the expression of human beta-like globin genes. *Mol. Cell. Biol.* **30**, 3460–3470.
- Morley, B.J., Abbott, C.A., Sharpe, J.A., Lida, J., Chan-Thomas, P.S., and Wood, W.G. (1992). A single beta-globin locus control region element (5' hypersensitive site 2) is sufficient for developmental regulation of human globin genes in transgenic mice. *Mol. Cell. Biol.* **12**, 2057–2066.
- Naumova, N., Imakaev, M., Fudenberg, G., Zhan, Y., Lajoie, B.R., Mirny, L.A., and Dekker, J. (2013). Organization of the mitotic chromosome. *Science* **342**, 948–953.
- Navas, P.A., Peterson, K.R., Li, Q., Skarpidi, E., Rohde, A., Shaw, S.E., Clegg, C.H., Asano, H., and Stamatoyannopoulos, G. (1998). Developmental specificity of the interaction between the locus control region and embryonic or fetal globin genes in transgenic mice with an HS3 core deletion. *Mol. Cell. Biol.* **18**, 4188–4196.
- Osborne, C.S., Chakalova, L., Brown, K.E., Carter, D., Horton, A., Debrand, E., Goyenechea, B., Mitchell, J.A., Lopes, S., Reik, W., and Fraser, P. (2004). Active genes dynamically colocalize to shared sites of ongoing transcription. *Nat. Genet.* **36**, 1065–1071.
- Palstra, R.J., Tolhuis, B., Splinter, E., Nijmeijer, R., Grosveld, F., and de Laat, W. (2003). The beta-globin nuclear compartment in development and erythroid differentiation. *Nat. Genet.* **35**, 190–194.
- Peterson, K.R., Navas, P.A., Li, Q., and Stamatoyannopoulos, G. (1998). LCR-dependent gene expression in beta-globin YAC transgenics: detailed structural studies validate functional analysis even in the presence of fragmented YACs. *Hum. Mol. Genet.* **7**, 2079–2088.
- Rao, S.S., Huntley, M.H., Durand, N.C., Stamenova, E.K., Bochkov, I.D., Robinson, J.T., Sanborn, A.L., Machol, I., Omer, A.D., Lander, E.S., and Aiden, E.L. (2014). A 3D map of the human genome at kilobase resolution reveals principles of chromatin looping. *Cell* **159**, 1665–1680.
- Sankaran, V.G., Xu, J., Byron, R., Greisman, H.A., Fisher, C., Weatherall, D.J., Sabath, D.E., Groudine, M., Orkin, S.H., Premawardhana, A., and Bender, M.A. (2011). A functional element necessary for fetal hemoglobin silencing. *N. Engl. J. Med.* **365**, 807–814.
- Schatz, P.J. (1993). Use of peptide libraries to map the substrate specificity of a peptide-modifying enzyme: a 13 residue consensus peptide specifies biotinylation in *Escherichia coli*. *Nat. Biotechnol.* **11**, 1138–1143.
- Schwartzman, O., Mukamel, Z., Oded-Elkayam, N., Olivares-Chauvet, P., Lubling, Y., Landan, G., Izraeli, S., and Tanay, A. (2016). UMI-4C for quantitative and targeted chromosomal contact profiling. *Nat. Methods* **13**, 685–691.
- Shao, Z., Zhang, Y., Yuan, G.C., Orkin, S.H., and Waxman, D.J. (2012). MAnorm: a robust model for quantitative comparison of ChIP-Seq data sets. *Genome Biol.* **13**, R16.
- Simonis, M., Klous, P., Splinter, E., Moshkin, Y., Willemsen, R., de Wit, E., van Steensel, B., and de Laat, W. (2006). Nuclear organization of active and inactive chromatin domains uncovered by chromosome conformation capture-on-chip (4C). *Nat. Genet.* **38**, 1348–1354.
- Stonestrom, A.J., Hsu, S.C., Jahn, K.S., Huang, P., Keller, C.A., Giardine, B.M., Kadauke, S., Campbell, A.E., Evans, P., Hardison, R.C., and Blobel, G.A. (2015). Functions of BET proteins in erythroid gene expression. *Blood* **125**, 2825–2834.
- Thurman, R.E., Rynes, E., Humbert, R., Vierstra, J., Maurano, M.T., Haugen, E., Sheffield, N.C., Stergachis, A.B., Wang, H., Vernot, B., et al. (2012). The accessible chromatin landscape of the human genome. *Nature* **489**, 75–82.
- Tolhuis, B., Palstra, R.J., Splinter, E., Grosveld, F., and de Laat, W. (2002). Looping and interaction between hypersensitive sites in the active beta-globin locus. *Mol. Cell* **10**, 1453–1465.
- Trapnell, C., Pachter, L., and Salzberg, S.L. (2009). TopHat: discovering splice junctions with RNA-Seq. *Bioinformatics* **25**, 1105–1111.
- van de Werken, H.J., Landan, G., Holwerda, S.J., Hoichman, M., Klous, P., Chachik, R., Splinter, E., Valdes-Quezada, C., Oz, Y., Bouwman, B.A., et al. (2012). Robust 4C-seq data analysis to screen for regulatory DNA interactions. *Nat. Methods* **9**, 969–972.
- Waldrip, Z.J., Byrum, S.D., Storey, A.J., Gao, J., Byrd, A.K., Mackintosh, S.G., Wahls, W.P., Taverna, S.D., Raney, K.D., and Tackett, A.J. (2014). A CRISPR-based approach for proteomic analysis of a single genomic locus. *Epigenetics* **9**, 1207–1211.



- Whyte, W.A., Orlando, D.A., Hnisz, D., Abraham, B.J., Lin, C.Y., Kagey, M.H., Rahl, P.B., Lee, T.I., and Young, R.A. (2013). Master transcription factors and mediator establish super-enhancers at key cell identity genes. *Cell* **153**, 307–319.
- Xu, J., Bauer, D.E., Kerenyi, M.A., Vo, T.D., Hou, S., Hsu, Y.J., Yao, H., Trowbridge, J.J., Mandel, G., and Orkin, S.H. (2013). Corepressor-dependent silencing of fetal hemoglobin expression by BCL11A. *Proc. Natl. Acad. Sci. USA* **110**, 6518–6523.
- Xu, J., Peng, C., Sankaran, V.G., Shao, Z., Esrick, E.B., Chong, B.G., Ippolito, G.C., Fujiwara, Y., Ebert, B.L., Tucker, P.W., and Orkin, S.H. (2011). Correction of sickle cell disease in adult mice by interference with fetal hemoglobin silencing. *Science* **334**, 993–996.
- Zhang, Y., Liu, T., Meyer, C.A., Eeckhoute, J., Johnson, D.S., Bernstein, B.E., Nusbaum, C., Myers, R.M., Brown, M., Li, W., and Liu, X.S. (2008). Model-based analysis of ChIP-Seq (MACS). *Genome Biol.* **9**, R137.
- Zhao, Z., Tavoosidana, G., Sjölander, M., Göndör, A., Mariano, P., Wang, S., Kanduri, C., Lezcano, M., Sandhu, K.S., Singh, U., et al. (2006). Circular chromosome conformation capture (4C) uncovers extensive networks of epigenetically regulated intra- and interchromosomal interactions. *Nat. Genet.* **38**, 1341–1347.
- Zhou, F., Lu, Y., Ficarro, S.B., Adelmant, G., Jiang, W., Luckey, C.J., and Marto, J.A. (2013). Genome-scale proteome quantification by DEEP SEQ mass spectrometry. *Nat. Commun.* **4**, 2171.